

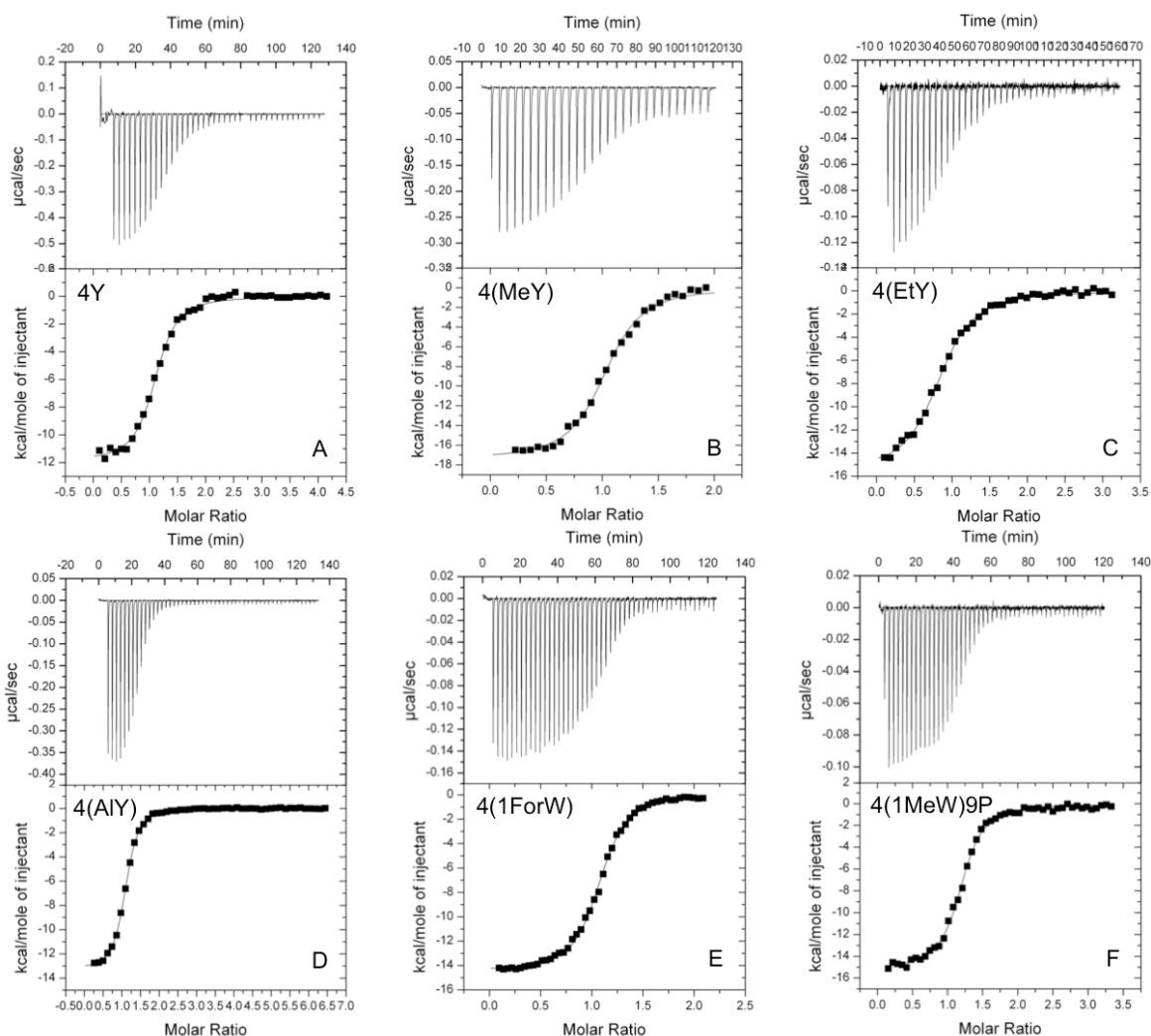
Magotti et al., Structure-Kinetic Relationships of Compstatin  
**Supplementary Table 1**

**Supp. Table 1:** LogP values of the side chains of amino acids used at position 4 of compstatin. All values were calculated using MolInspiration ([www.molinspiration.com](http://www.molinspiration.com))

<b>Amino Acid</b>	<b>logP</b>
W	2.53
1MeW	2.60
1ForW	2.41
5MeW	2.96
Y	1.90
MeY	2.44
EtY	2.81
AlY	3.87
2Nal	3.57
PyrA	5.20

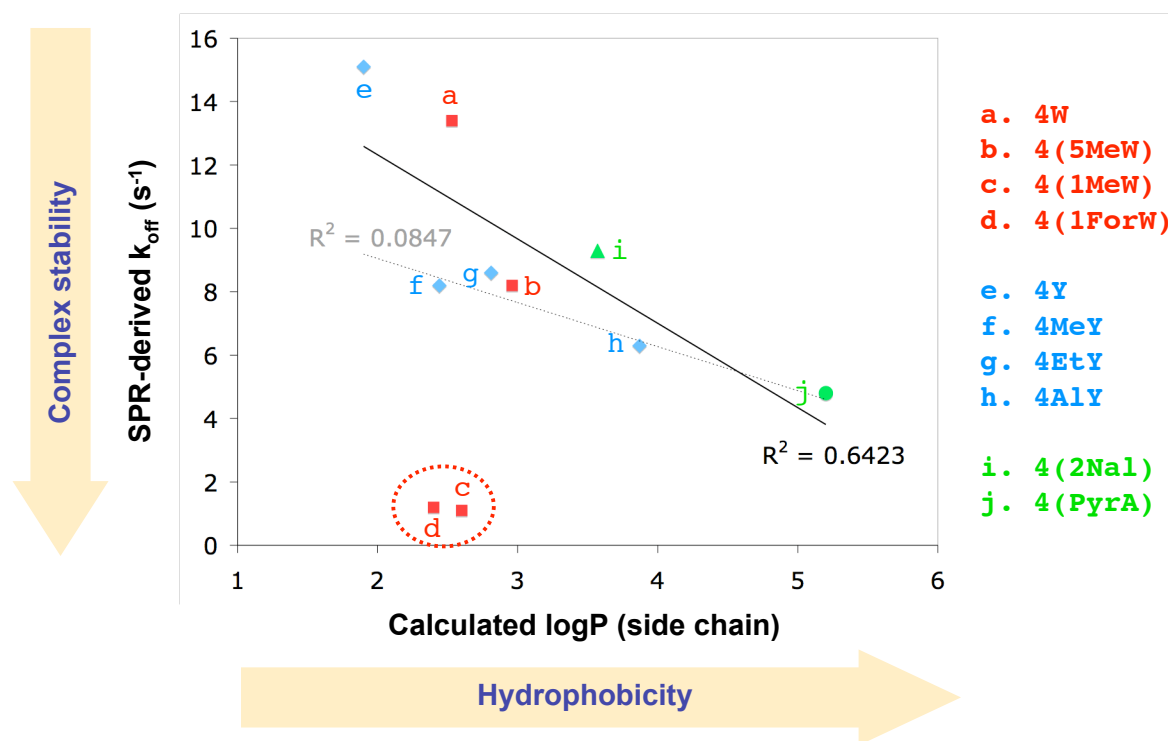
# Magotti et al., Structure-Kinetic Relationships of Compstatin

## Supplementary Figure 1



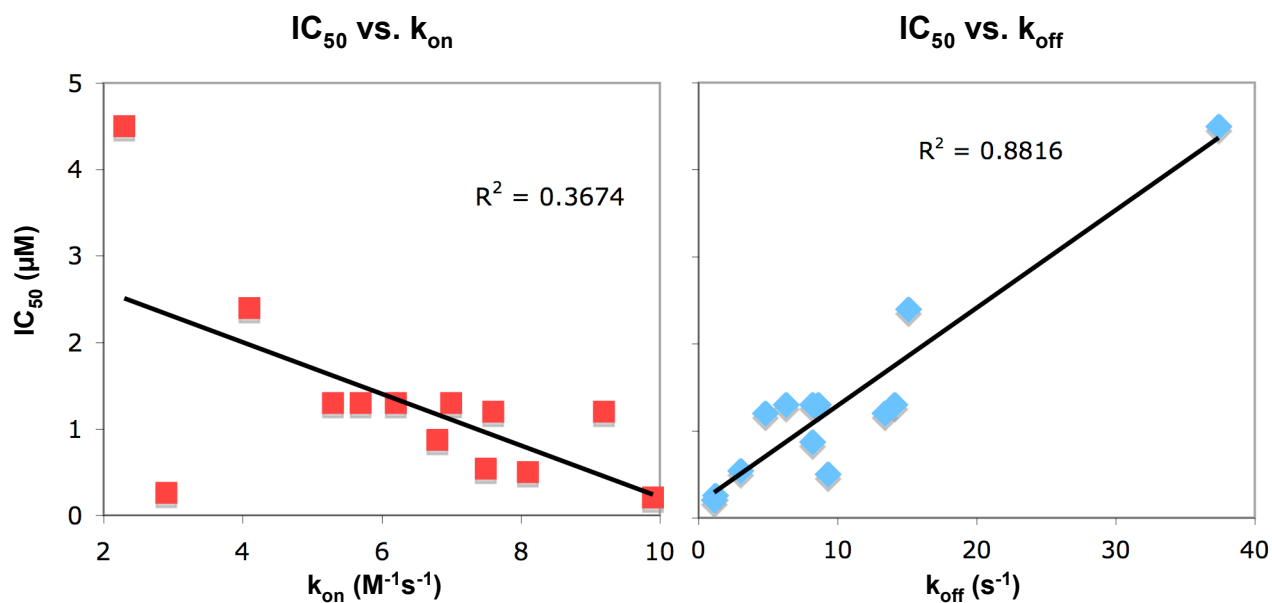
**Supp. Fig. 1:** ITC profiles representing the interaction of 4Y (A), 4(MeY) (B), 4(EtY) (C), 4(AIY) (D), 4(1ForW) (E) and 4(1MeW)9P (F) with C3. Isotherms represent binding at 25 °C and were corrected for heats of dilution (upper panels). The plots were obtained by fitting the raw data with a 'one set of sites' model using Origin 7.0 (lower panels). The analog 4(PyrA) could not be tested due to poor solubility at the high concentrations required for ITC experiments.

Magotti et al., Structure-Kinetic Relationships of Compstatin  
**Supplementary Figure 2**



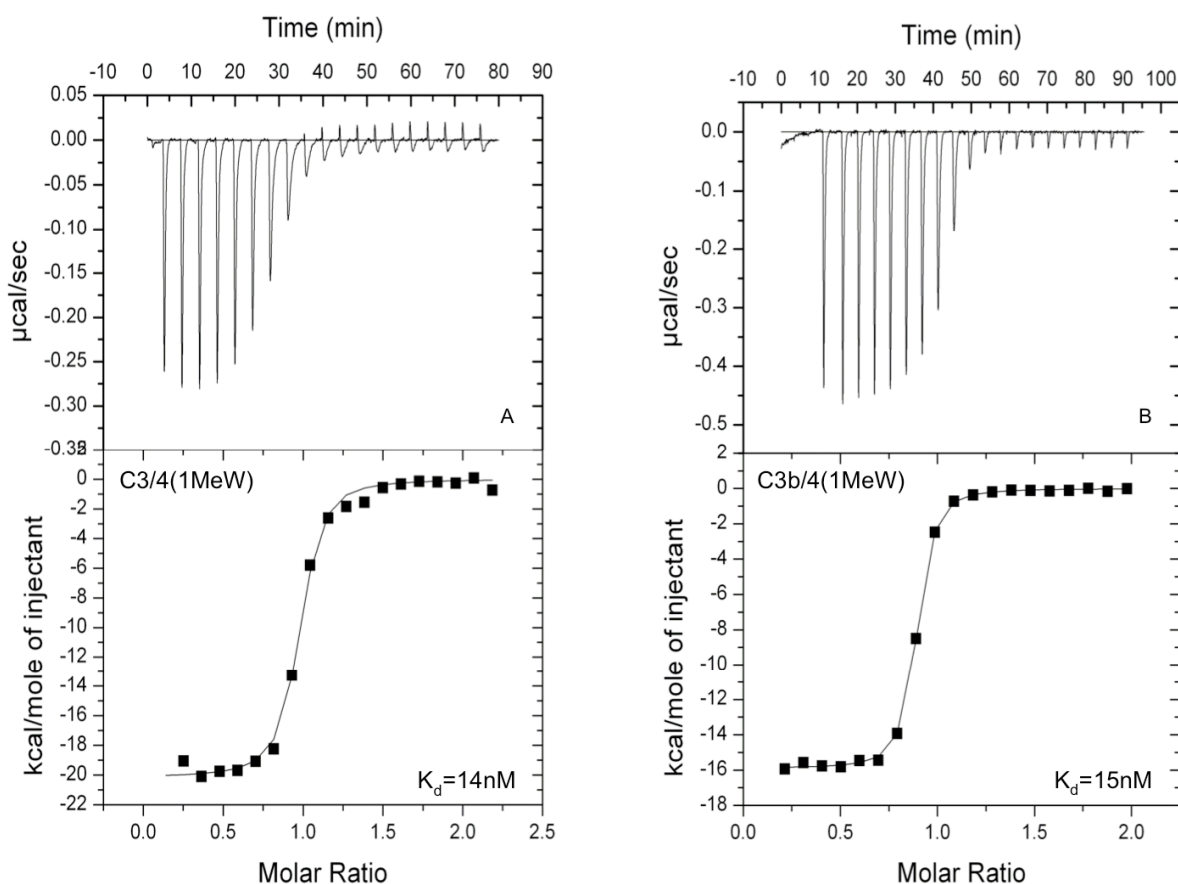
**Supp. Fig. 2:** Correlation between the dissociation rate constant ( $k_{off}$ ) from SPR profiling and the calculated hydrophobicity ( $\log P$ ) of peptides with modification at position 4. Tryptophan analogs (a-d) are marked in red, tyrosine derivatives (e-h) in blue and bulky aromatic substituents (j-j) in green. While the entire data set shows only a weak linear correlation (dotted line;  $R^2 = 0.08$ ), this trend is dramatically improved when the two indol N-derivatives (1MeW, 1ForW) are removed (solid line;  $R^2 = 0.64$ ). This indicates that an increase in hydrophobicity indeed has a positive effect on protein stability. However, individual mutations may have a more dramatic effect and therefore largely exceed the predicted trend, most likely by forming specific and strong contacts with residues within the compstatin binding site on C3b. A similar yet much less pronounced effect is observed for MeY, which is significantly more stable than the  $\log P$  trend between tyrosine derivatived would have suggested. All  $\log P$  values were calculated for the side chain of residue 4 using MolInspiration ([www.molinspiration.com](http://www.molinspiration.com)) and are listed in Supplementary Table 1).

Magotti et al., Structure-Kinetic Relationships of Compstatin  
**Supplementary Figure 3**



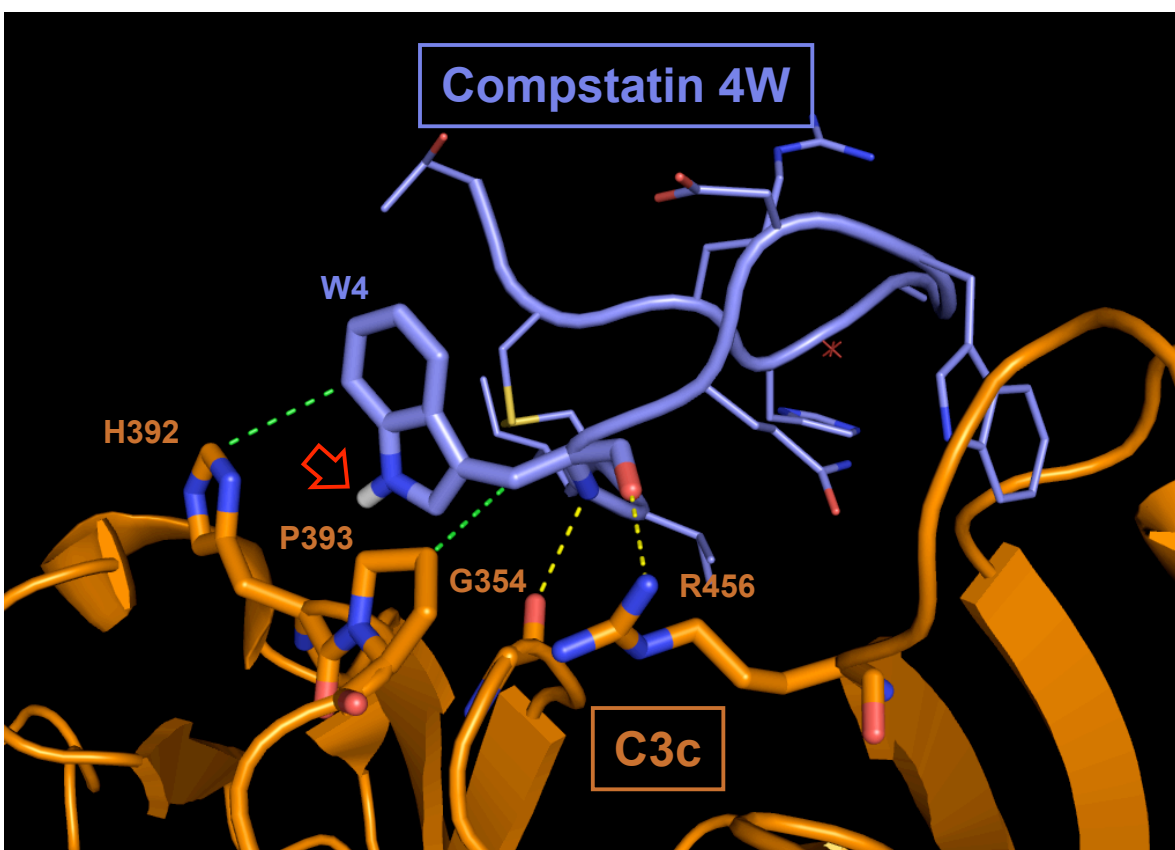
**Supp. Fig. 3:** Correlation between activities from the complement inhibition assay (IC<sub>50</sub>) and the kinetic on-rates (left) and off-rates (right) from the SPR profiling. Though both plots show a linear trend over the entire data set, the correlation is higher and more consistent in case of k<sub>off</sub>. This is most likely a result of the differences in the assay format: ELISA-based assays are generally more linked to the off-rate, as they depend on the complex stability during wash steps and for the end-point measurement.

Magotti et al., Structure-Kinetic Relationships of Compstatin  
**Supplementary Figure 4**



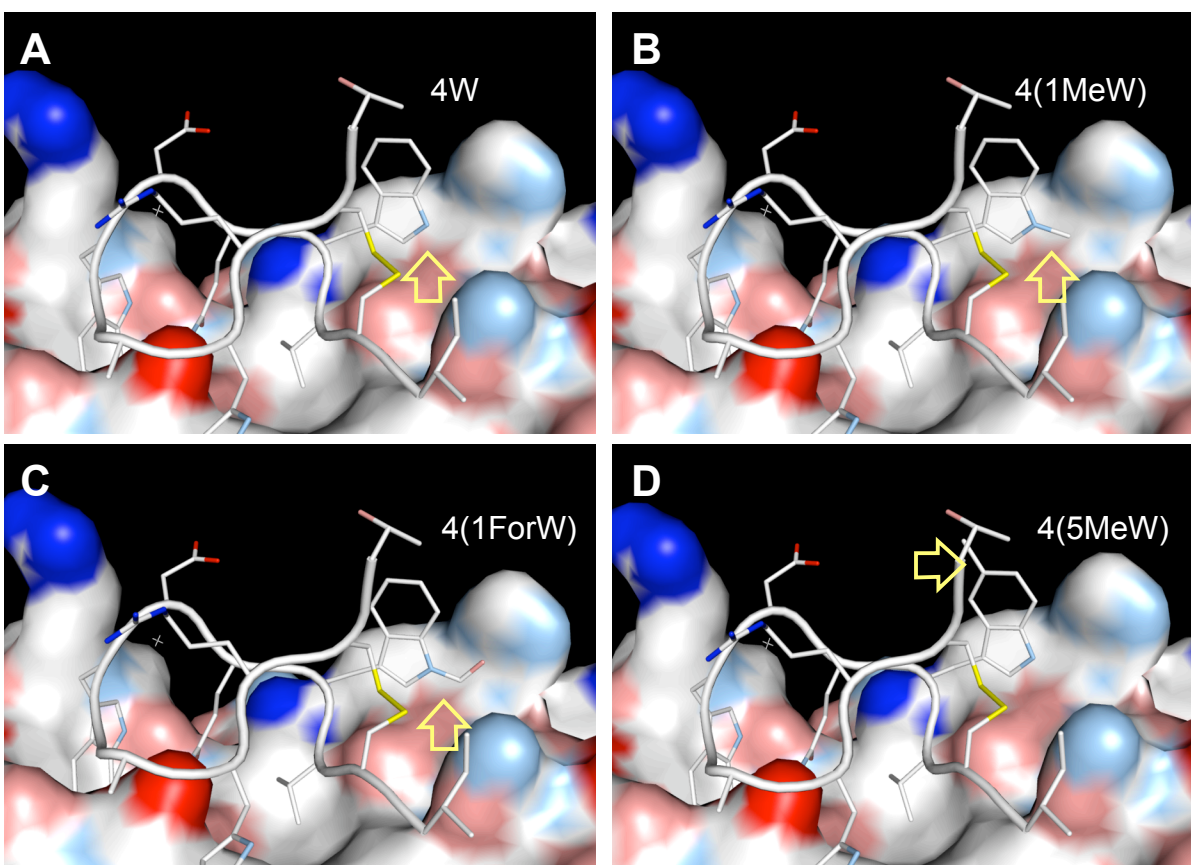
**Supp. Fig. 4:** Thermodynamic characterization and comparison of analog 4(1MeW) binding to C3 (A) and C3b (B) using ITC. Due to technical reasons (protein concentration, immobilization methods) and comparability with previous data (Katragadda et al., 2006), C3 was used in all ITC and C3b in all SPR experiments. As the binding site of compstatin is located in the stable part of the C3  $\beta$ -chain (MG4/MG5 domains), which is conserved between C3, C3b, and C3c (Janssen et al., 2007), no significant difference are expected for the binding mode of the inhibitor. Indeed, the extracted binding affinity ( $K_D$ ) was highly similar for both C3 and C3b, therefore confirming the homology of the binding site and validating the comparability of the ITC and SPR affinities.

Magotti et al., Structure-Kinetic Relationships of Compstatin  
**Supplementary Figure 5**



**Supp. Fig. 5:** Contact network between Trp-4 of compstatin analog 4W (blue) and C3c as reported for the co-crystal structure (Janssen et al., 2007). Two hydrogen bonds (yellow dashed lines) between the backbone of Trp-4 and Glu-354 and Arg-456 of C3c, as well as two hydrophobic contacts (green dashed lines) between C7 (indole ring) and C8 (methylene) of Trp-4 and His-392 and Pro-393 of C3c, respectively. No contacts are reported for the indole nitrogen (red arrow; depicted with hydrogen atom).

Magotti et al., Structure-Kinetic Relationships of Compstatin  
**Supplementary Figure 6**



**Supp. Fig. 6:** Molecular modeling of compstatin analogs with modifications at tryptophan 4. **(A)** The indole nitrogen of analog 4W points towards a primarily hydrophobic cleft formed by residues 390-393 of C3c. **(B)** Replacement of the indole N-hydrogen by a methyl group leads to analog 4(1MeW). The methyl group points directly into the spacious cleft. **(C)** While the carbon atom of the formyl group in analog 4(1ForW) is considered being at the same position as in case of 4(1MeW), the orientation of the carbonyl-O may vary. **(D)** When the methyl group is added at position 5 of tryptophan (i.e. analog 4(5MeW)), the methyl carbon sticks out into the solvent and is not likely to undergo any direct contacts. All modifications were performed on the co-crystal structure derived from PDB file 2QKI (Janssen et al., 2007) using PyMOL ([www.pymol.org](http://www.pymol.org)). Compstatin is represented as ribbon with side chains as sticks; C3c is shown as a solvent-accessible surface. Both structures are colored as following: white = non-polar, pale blue = polar N, pale red = polar O, dark blue = charged N, dark red = charged O.